



## Review

Relevance of rhodopsin studies for GPCR activation<sup>☆</sup>Xavier Deupi<sup>\*</sup>

Condensed Matter Theory Group and Laboratory of Biomolecular Research, Paul Scherrer Institute, WHGA/106, CH-5232 Villigen PSI, Switzerland

## ARTICLE INFO

## Article history:

Received 25 July 2013

Received in revised form 2 September 2013

Accepted 5 September 2013

Available online 13 September 2013

## Keywords:

Rhodopsin

G protein-coupled receptors

GPCR activation

Structural biology

Structural bioinformatics

## ABSTRACT

Rhodopsin, the dim-light photoreceptor present in the rod cells of the retina, is both a retinal-binding protein and a G protein-coupled receptor (GPCR). Due to this conjunction, it benefits from an arsenal of spectroscopy techniques that can be used for its characterization, while being a model system for the important family of Class A (also referred to as “rhodopsin-like”) GPCRs. For instance, rhodopsin has been a crucial player in the field of GPCR structural biology. Until 2007, it was the only GPCR for which a high-resolution crystal structure was available, so all structure–activity analyses on GPCRs, from structure-based drug discovery to studies of structural changes upon activation, were based on rhodopsin. At present, about a third of currently available GPCR structures are still from rhodopsin. In this review, I show some examples of how these structures can still be used to gain insight into general aspects of GPCR activation. First, the analysis of the third intracellular loop in rhodopsin structures allows us to gain an understanding of the structural and dynamic properties of this region, which is absent (due to protein engineering or poor electron density) in most of the currently available GPCR structures. Second, a detailed analysis of the structure of the transmembrane domains in inactive, intermediate and active rhodopsin structures allows us to detect early conformational changes in the process of ligand-induced GPCR activation. Finally, the analysis of a conserved ligand-activated transmission switch in the transmembrane bundle of GPCRs in the context of the rhodopsin activation cycle, allows us to suggest that the structures of many of the currently available agonist-bound GPCRs may correspond to intermediate active states. While the focus in GPCR structural biology is inevitably moving away from rhodopsin, in other aspects rhodopsin is still at the forefront. For instance, the first studies of the structural basis of disease mutants in GPCRs, or the most detailed analysis of cellular GPCR signal transduction networks using a systems biology approach, have been carried out in rhodopsin. Finally, due again to its unique properties among GPCRs, rhodopsin will likely play an important role in the application of X-ray free electron laser crystallography to time-resolved structural biology in membrane proteins. Rhodopsin, thus, still remains relevant as a model system to study the molecular mechanisms of GPCR activation. This article is part of a Special Issue entitled: Retinal Proteins—You can teach an old dog new tricks.

© 2013 Elsevier B.V. All rights reserved.

## 1. Introduction

Thanks to innovative protein engineering techniques and crystallography methods [1,2], from 2007 there has been an almost exponential growth in the number of available G protein-coupled receptor (GPCR) structures [3]. While this has provided unprecedented insights into the structural and functional diversity of this protein family, it is becoming increasingly more difficult to identify common features that allow us to derive the general aspects of GPCR function. This is especially true as most of these new structures have required heavy protein engineering to yield crystallizable proteins, such as removal of post-translational modifications, truncations of flexible regions, creation of fusion chimeras, addition of thermostabilizing mutations or the use of antibodies. The only exception is still rhodopsin, which has been crystallized with its full sequence including the third intracellular loop and the

C-terminus, and in a native form or with minimal modifications. Rhodopsin is also remarkable in other aspects. For instance, all Class A non-rhodopsin GPCR structures so far have been solved by molecular replacement and are thus ultimately based on the first structure of rhodopsin [4]. Rhodopsin further yielded the first structure of a recombinant GPCR produced in mammalian cells, and the first solved using microcrystallographic techniques. The combination of these two factors opened the revolution in GPCR structural biology that we are experiencing nowadays.

There are currently 25 structures of eukaryotic rhodopsins deposited in the Protein Data Bank (Table 1), which account roughly to 1/3 of all the GPCR structures available. The majority of these structures (21) are from bovine rhodopsin. Of these, 10 correspond to inactive states (i.e. dark states bound to 11-*cis* or 9-*cis* retinal), 8 correspond to active states (light-activated or obtained by soaking all-*trans* retinal in opsin crystals) and, importantly, 3 structures correspond to activation intermediates (bathorhodopsin, lumirhodopsin and a deprotonated intermediate). There is also a low resolution electron density map of an additional intermediate, metarhodopsin I [5]. In addition, there are 4

<sup>☆</sup> This article is part of a Special Issue entitled: Retinal Proteins—You can teach an old dog new tricks.

<sup>\*</sup> Tel.: +41 56 310 3337.

**Table 1**  
Crystal structures of rhodopsin (2000–2013).

Dark-state (inactive)							
Bovine							
PDB id	Publication	Resolution	Construct	retinal	Cytoplasmic partner	Comments	Reference
1F88	2000	2.80	WT	11- <i>cis</i>	–		Palczewski et al. (2000). Science, 289(5480), 739–745
1HZX	2001	2.80	WT	11- <i>cis</i>	–		Teller et al. (2001). Biochemistry, 40(26), 7761–7772
1L9H	2002	2.60	WT	11- <i>cis</i>	–		Okada et al. (2002). PNAS, 99(9), 5982–5987
1U19	2004	2.20	WT	11- <i>cis</i>	–		Okada et al. (2004). J Mol Biol, 342(2), 571–583
1GZM	2004	2.65	WT	11- <i>cis</i>	–		Li et al. (2004). J Mol Biol, 343(5), 1409–1438
2135	2006	3.80	WT	11- <i>cis</i>	–		Salom et al. (2006). PNAS, 103(44), 16123–16128
2136	2006	4.10	WT	11- <i>cis</i>	–		Salom et al. (2006). PNAS, 103(44), 16123–16128
2J4Y	2007	3.40	N2C/D282C	11- <i>cis</i>	–	First structure of a recombinant GPCR	Standfuss et al. (2007). J Mol Biol, 372(5), 1179–1188
2PED	2007	2.95	WT	9- <i>cis</i>	–		Sekharan et al. (2007). JACS, 129(5), 1052–1054
3OAX	2010	2.60	WT	11- <i>cis</i>	–	+ $\beta$ -Ionone (allosteric site)	Makino et al. (2010). Biophys J, 99(7), 2366–2373
SQUID							
2Z1Y		3.70	WT	11- <i>cis</i>	–		Shimamura et al. (2008). J Biol Chem, 283(26), 17753–17756
2Z73		2.50	WT	11- <i>cis</i>	–		Murakami et al. (2008). Nature, 453(7193), 363–367
3AYN		2.70	C-terminally truncated	9- <i>cis</i>	–		Murakami et al. (2011). J Mol Biol, 413(3), 615–627
Light-activated (activation intermediates)							
Bovine							
2137	2006	4.15	WT	All- <i>trans</i>	–	Deprotonated intermediate	Salom et al. (2006). PNAS, 103(44), 16123–16128
2G87	2006	2.60	WT	All- <i>trans</i>	–	Bathorhodopsin	Nakamichi et al. (2006). Angew Chem Int Ed, 45(26), 4270–4273
2HPY	2006	2.80	WT	All- <i>trans</i>	–	Lumirhodopsin	Nakamichi et al. (2006). PNAS, 103(34), 12729–12734
Squid							
3AYM	2011	2.80	C-terminally truncated	All- <i>trans</i>	–	Bathorhodopsin	Murakami et al. (2011). J Mol Biol, 413(3), 615–627
Light-activated (active)							
Bovine							
3CAP	2008	2.90	WT	–	–	Opsin	Park et al. (2008). Nature, 454(7201), 183–187
3DQB	2008	3.20	WT	–	G $\alpha$ CT	Opsin	Scheerer et al. (2008). Nature, 455(7212), 497–502
2X72	2011	3.00	N2C/D282C/E113Q	All- <i>trans</i>	G $\alpha$ CT	Constitutively active mutant	Standfuss et al. (2011). Nature, 471 (7340), 656–660
3PQR	2011	2.85	WT	All- <i>trans</i>	G $\alpha$ CT2	Opsin soaked with all-trans retinal	Choe et al. (2011). Nature, 471(7340), 651–655
3PXO	2011	3.00	WT	All- <i>trans</i>	–	Opsin soaked with all-trans retinal	Choe et al. (2011). Nature, 471(7340), 651–655
4A4M	2012	3.30	N2C/D282C/M257Y	All- <i>trans</i>	G $\alpha$ CT	Constitutively active mutant	Deupi et al. (2012). PNAS, 109(1), 119–124
4BEY	2013	2.90	N2C/D282C/G90D	All- <i>trans</i>	G $\alpha$ CT	Constitutively active mutant	Singhal et al. (2013). EMBO reports, 14(6), 520–526
4BEZ	2013	3.30	N2C/D282C/G90D	All- <i>trans</i>	–	Constitutively active mutant	Singhal et al. (2013). EMBO reports, 14(6), 520–526

structures of squid rhodopsin: 3 inactive and one intermediate active state (bathorhodopsin). Thus, rhodopsin is the GPCR for which we possess a richer structural information about the activation intermediates, and much can be learned about the general aspects of GPCR activation by analyzing these structures.

Identification of structural intermediates has been aided by the detailed spectroscopic characterization of the rhodopsin activation cycle by UV–VIS and FTIR spectroscopy (see [6] for a review). Once identified, rhodopsin intermediate states can be stabilized by, for instance, adjusting temperature and pH, which allowed their characterization using a variety of techniques (e.g. site-directed labeling methods coupled with spin-labeling EPR [7], double electron–electron resonance (DEER) [8] or fluorescence [9] spectroscopy) and, ultimately, their crystallization and structure determination [10–12]. NMR spectroscopy in GPCRs was also pioneered in rhodopsin. For instance, solid-state NMR has been used to characterize conformational changes in the retinal binding pocket [13] and in the cytoplasmic side of rhodopsin [14], or the dynamic properties of retinal [15] during different states in the activation process (see [16] for a review).

The possibility to trigger activation by photoisomerization of retinal allows a fine control in the experimental set-up of such assays. Such property, however, is not strictly restricted to rhodopsin, as there exist “caged” compounds (e.g. 2-nitrobenzyl derivatives of adrenergic ligands [17,18]) that can be converted into agonists using light. Thus, photoactivation of non-rhodopsin GPCRs, in combination with, for instance, FTIR or NMR spectroscopy (as it has been done in the glutamate receptor [19],  $\text{Ca}^{2+}$ -ATPase [20] and Ras [21]), could also be used in the future to monitor ligand-induced conformational changes in a wider range of GPCRs. However, non-rhodopsin GPCR intermediate states are usually stabilized using pharmacological tools (e.g. inverse, partial or biased agonists). In recent years, some aspects of such conformational states in the  $\beta_2$  adrenergic receptor, such as ligand-specific structural changes around in the extracellular domains [22], structural plasticity in transmembrane helix 6 (TM6) and TM7 related to biased agonism [23], and the existence of conformational states not observed in crystal structures [24,25], have been characterized by NMR spectroscopy.

The unique properties of rhodopsins make them valuable systems to study the molecular details of intermediates in the GPCR activation pathway. In this review, I will discuss three examples of how rhodopsin structures can be used to gain insight into general aspects of the dynamics of GPCR activation. First, the analysis of the third intracellular loop in bovine rhodopsin structures allows us to gain insight into the flexibility and dynamic properties of this region, absent in most of the available GPCR structures. Comparison with squid rhodopsin and human adenosine  $\text{A}_{2\text{A}}$  receptor suggests the presence of secondary structure in the N- and C-terminal domains of this loop. Second, a detailed structural analysis of TM2 and TM3 in inactive, intermediate and active rhodopsin structures allows us to detect early conformational changes that constitute the first steps in an activation pathway through TM7, and may be related to the phenomenon of biased signaling in non-rhodopsin GPCRs. Finally, the analysis of a conserved feature of agonist-bound GPCR structures (activation of a transmission switch in the TM3–TM5–TM6 interface) in the context of the rhodopsin activation cycle, allows us to suggest that these structures may correspond to intermediate active states.

## 2. Structure of the third intracellular loop in GPCR crystal structures

The third intracellular loop (ICL3), joining the cytoplasmic sides of TM5 and TM6 and involved in binding and activation of cytoplasmic partners, is highly variable in length in human rhodopsin-like GPCRs ( $126 \pm 114$  amino acids [26]). In many receptors, this region is likely intrinsically disordered [27], which would allow regulation of protein–protein recognition by exposure of linear peptide motifs [28]. Such long and flexible regions may preclude formation of ordered protein crystals and, thus, despite their functional relevance, they are often

engineered for structural studies. For instance, in many GPCR constructs for crystallography, ICL3 was substituted by a conformationally stable soluble protein (T4 lysozyme [29] or apocytochrome b(562)RIL [30]). While these fusion proteins have paved the way for the great recent advances in GPCR crystallography, they inherently mask the structural and functional properties of the cytoplasmic side of the receptor. As an alternative strategy, in some receptors ICL3 has been truncated to reduce the conformational heterogeneity of the protein construct. While initially these shortened loops featured very low electron density, more recent structures have been able to solve its structure, e.g. in the  $\beta_1$  [31] and  $\beta_2$  adrenergic receptors [32] (Fig. 1). Interestingly, in the case of the  $\beta_1$  adrenergic receptor, two distinct conformations of the cytoplasmic side of TM6 and ICL3 were observed, which has been suggested to be involved in the basal activity of the receptor [31]. The most compelling evidence of the role of ICL3 in the interaction with intracellular partners comes from the crystal structure of the complex between the  $\beta_2$  adrenergic receptor and Gs [33]. The receptor construct contains the full ICL3 sequence (54 residues [34]), which, in the crystal structure, forms a helical extension of TM5 (~3 helix turns) and TM6 (~4 helix turns) joined by a disordered (and not visible) stretch of 26 amino acids. In this case, the resolved region of TM5 protrudes ~21 Å into the cytoplasm, similarly to squid rhodopsin or the  $\text{A}_{2\text{A}}$  receptor (Fig. 1).

To date, only three GPCRs have been solved with a visible native full-length ICL3: bovine and squid rhodopsin (see Table 1) and the adenosine  $\text{A}_{2\text{A}}$  receptor [35,36] (Fig. 1).

The structures of inactive dark-state bovine rhodopsin provide valuable information about the putative structural flexibility of ICL3. While this loop is relatively short (26 residues; Leu226–Thr251 [34]), it features two different conformations. In the trigonal crystal form (PDB id: 1GZM, 2J4Y, 2I35 and 2I36), TM5 and TM6 extend 10 and 16 Å respectively into the cytoplasm, and are joined by a short 11 residue “arch” (Fig. 1). On the other hand, in the tetragonal crystal form TM5 only extends 6 Å into the cytoplasm, and the unstructured segment joining the helices “folds back” towards the membrane. In both crystal forms, ICL3 points into a solvent channel and is not responsible for crystal packing. Also, the high B-factors of this region have been proposed to correspond

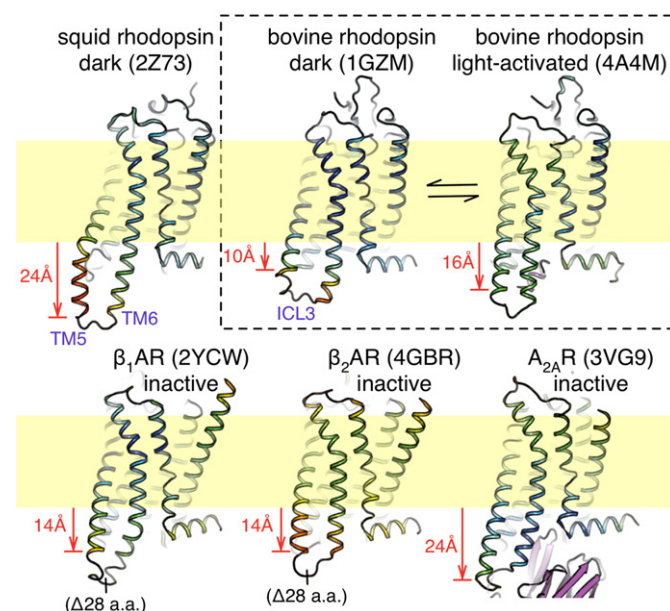


**Fig. 1.** GPCR crystal structures with solved ICL3. In the  $\beta_1$  and  $\beta_2$  adrenergic receptors the loop was truncated for crystallography, while squid and bovine rhodopsin, and the adenosine  $\text{A}_{2\text{A}}$  receptor feature the full-length native loop. In all cases, most of ICL3 forms an extension of TM5 and TM6, that can extend up to 24 Å into the cytoplasm. The structures of dark (inactive) and light-activated (active) rhodopsin (boxed) allow the visualization of the conformational changes in this loop associated to receptor activation.

to authentic indicators of main chain flexibility [37]. Thus, it is likely that these conformations result from the inherent structural flexibility of ICL3, and can be present in a biological environment. Upon activation, the cytoplasmic side of TM5 straightens and elongates approximately 6 additional Å (Fig. 1, box), resulting in a marked shortening of stretch joining the helical segments of ICL3. This active conformation of ICL3 is common to the structures of active opsin at low pH, active opsin soaked with all-*trans* retinal and light-activated rhodopsin mutants, in the presence and absence of stabilizing GαCT peptides. Thus, it seems likely that these new structures of ICL3 correspond to the biological conformation in the Meta II active state.

The structure of squid rhodopsin [38] revealed that TM5 and TM6 could prolong even further beyond the cell membrane. In this case, the longer ICL3 (32 residues) extends 24 Å into the cytoplasm, as two helical stretches of ~4 turns joined by a short stretch of ~6 residues (Fig. 1). Such fold is also present in several recent structures of the A<sub>2A</sub> receptor (thermostabilized by alanine mutagenesis [35] and bound to an allosteric inverse agonist antibody [36]) (Fig. 1), although in a slightly different orientation. Thus, despite that we still have a limited structural information about this region, it seems likely that the helical segments forming N- and C-terminal parts of ICL3 (i.e. the extensions of TM5 and TM6 into the cytoplasm) are a common feature among GPCRs. Interestingly, an NMR structure of ICL3 of the vasopressin V2 receptor [39] shows that this “loop” also is formed by two long alpha helices, which are proposed to be extensions of TM5 and TM6 that protrude into the cytoplasm, joined by a short arginine-rich loop of higher mobility.

In summary, ICL3 is key to understand the structural basis of the interaction between GPCRs and intracellular partners (e.g. G proteins, kinases and arrestins). Currently, our knowledge of full-length native ICL3 structures is limited to rhodopsins and, recently, the A<sub>2A</sub> receptor. These structures, thus, constitute valuable templates for homology modeling of ICL3, either in receptors of unknown structure, or in currently available structures where this loop has been substituted by a fusion partner. It is important to remember that in many cases ICL3 can be much longer than in the available templates: e.g. 150–200 residues in the recently crystallized M2 [40] and M3 [41] muscarinic receptors. In addition, these long loops can be intrinsically disordered [42]. Despite these drawbacks, our current knowledge of the structure of ICL3 can still be used to gain insight into the details of GPCR activation, particularly in receptors of relatively short (<50 residues) ICL3 (e.g. V2 vasopressin or neurotensin NTS1 receptors). For instance, the NMR structure of ICL3 of the V2 vasopressin receptor [39] and the structure of squid rhodopsin [38] were used to model the cytoplasmic region of the vasopressin V2 receptor and interpret fluorescence spectroscopy data to gain insight into the structural basis of biased signaling [43].

### 3. Early conformational changes in GPCR activation

The crystal structures of rhodopsin revealed that the transmembrane segments in GPCRs were far from being ideal α-helices. Also, while the presence of highly conserved Pro residues in TM5, TM6 and TM7 suggested that these helices were kinked, they do not resemble “standard” Pro-kinked helices either, but present very strong localized structural distortions [44]. Among the methods to quantify distortions in protein structures, HelAnal [45] provides local bend and opening/tightening (twist) values for each helix turn.

Fig. 2 shows the profiles of helix bend and twist for TM2 and TM3 in the structures of inactive (red), bathorhodopsin and lumirhodopsin (orange) and active (yellow) states of rhodopsin. While TM3 is a fairly regular α-helix (unit twist around 100° and low local bend angles), TM2 presents a strong bend and helix opening (decrease in unit twist) at Gly89(2.56)–Gly90(2.57) (the numbers in parenthesis denote the residue position in the Ballesteros–Weinstein scheme [46]). In the inactive state, this local distortion is stabilized by an unusual intrahelical hydrogen bond network [47] and possibly by a water molecule, as

observed in the structure of lumirhodopsin [11]. This local distortion is translated in an overall bend of ~30° in TM2 towards TM1 and away from TM3 [37].

Upon light activation, retinal isomerization results in an increase in the volume of the binding pocket, already in lumirhodopsin, primarily due to the relocation of the Met207(5.42) side chain [48]. However, the most noticeable structural changes in the backbone occur in TM2 (around Gly89(2.56)–Gly90(2.57)) and TM3 (around G114(3.29) and G120(3.35)–G121(3.36)) [11] in the transition from bathorhodopsin to lumirhodopsin (Fig. 2). These structural changes can be visualized as a local increase in the helix bend (10–20°) in TM2 and TM3 (compare red vs. orange lines). In both cases, these distortions relax in the transition to the Meta II state (compare orange vs. yellow lines). The local structural rearrangement at the backbone of Gly89(2.56)–Gly90(2.57) in lumirhodopsin also correlates with the change of the side chain conformation of Met86(2.53). In human rhodopsin-like GPCRs, position 2.53 contains 81% of bulky/aromatic residues. In addition, an evolutionary trace analysis in rhodopsin-like GPCRs identified Met86(2.53) in the top 20% of important conserved positions [49]. Application of this technique to bioamine receptors leads us to suggest that this position may communicate with Trp(6.48) through intervening water molecules that occupy a cavity in the structure [50]. Thus, the early structural changes in TM2 at the level of the binding pocket observed in the lumirhodopsin state, together with the change in the side chain conformation of Met86(2.53), may be the first stage of an activation pathway through TM2/TM7 [51], which is amplified in later stages. In Meta II, the larger movements in TM6 and TM7 weaken the packing between TM2, TM3, TM6 and TM7, mediated by Met86(2.53), Gly121(3.36), Trp265(6.48) and Ser298(7.45), which opens a passage connecting the ligand binding pocket to the cytoplasmic side of the transmembrane bundle (Fig. 3) [52]. This, combined with the opening of a cytoplasmic hydrophobic barrier [53], allows the relocation of a cluster of intramolecular water molecules, which creates a new set of hydrogen bond interactions that stabilize the active state. Relocation of these waters is directly translated into a remarkable conformational change in TM7, a key feature of the active state.

While Gly89(2.56)–Gly90(2.57) are conserved only in rhodopsin vertebrate type 1 GPCRs, other rhodopsin-like GPCRs feature Pro residues at the 2.57, 2.58, 2.59 and 2.60 positions with different patterns of conservation in different subfamilies [47]. In the currently available crystal structures, a variety of sequence motifs stabilize different local structures that are key to shape the binding pocket. Interestingly, the extracellular side of TM2 is key for ligand-induced activation in several GPCRs, and has been suggested to be involved in biased signaling [54]. Thus, while some aspects of the above activation mechanism may be specific to rhodopsin, the existence of a signal transduction pathway that connects ligand-induced local conformational changes in TM2 (as observed in lumirhodopsin) with larger structural changes in TM7 may be a conserved feature of rhodopsin-like GPCRs.

### 4. Structures of agonist-bound GPCRs as intermediates in the activation pathway

GPCRs exist not only in a dual inactive/active state, but in an ensemble of conformations [55], which, in many cases, contains a small population of active states even in the absence of activating signals [56]. Activation can then be depicted as shifts in the population of these discrete conformational intermediates [57]. In several GPCRs, such intermediates have been detected by, for instance, fluorescence spectroscopy [43,56], NMR [24] or fluorescence resonance energy transfer [58]. However, most of our knowledge of the intermediate states in GPCR activation has originated from rhodopsin (see [6] for a comprehensive review), where such metastable intermediates can be characterized by spectroscopic methods (UV–VIS and FTIR spectroscopy). The crystal structures of bathorhodopsin [10,12], lumirhodopsin [11] and the electron crystallography map of Meta I [5] revealed that there



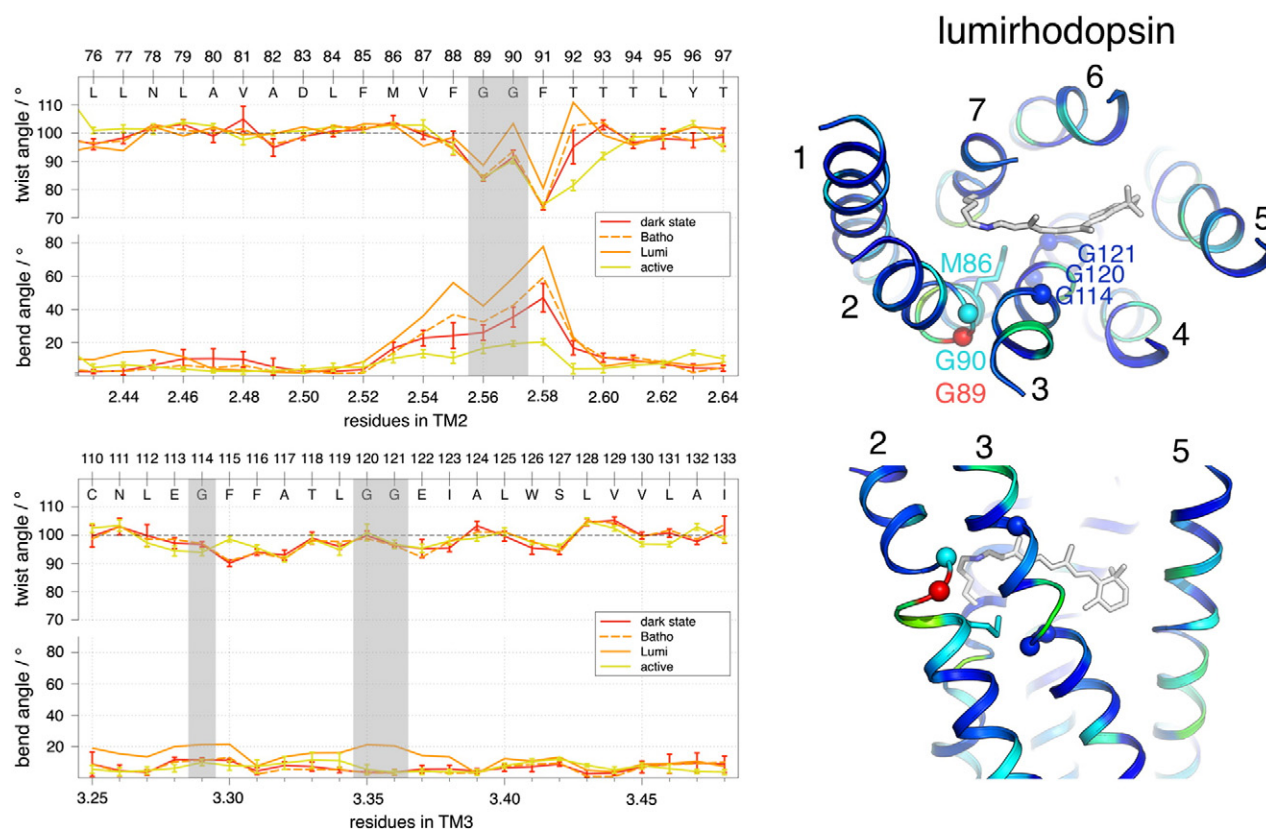


**Fig. 2.** Left panel: local bend and unit twist profiles for TM2 (top) and TM3 (bottom) in the crystal structures of rhodopsin. The horizontal black line in the twist profiles depicts the value for an ideal  $\alpha$ -helix ( $100^\circ$ ). A decrease in twist corresponds to a local opening in the helix. The strongest distortions and changes upon activation are localized near the Gly residues in these helices (gray boxes). Right panel: difference in local bend between dark inactive rhodopsin and lumirhodopsin plotted on the structure of lumirhodopsin (blue—no difference; red—highest difference). The main structural changes in the early stages of activation are found at the Gly89(2.56)–Gly90(2.57) motif in TM2, and near Met86(2.53) (blue sticks), which changes conformation during the transition to the lumirhodopsin state.

are no major structural changes in these early intermediates, but only small local rearrangements in the retinal binding site. Also, an FTIR spectroscopy analysis of rhodopsin incorporating genetically encoded infrared probes [59] shows only small-scale structural changes in the cytoplasmic side in the transition from Lumi to Meta I, consisting in a rotation of TM6 and a movement of TM5 away from TM3. The structures of rhodopsin in an active conformation [52,53,60–63] have shown the larger-scale conformational rearrangements related to the transition to the Meta II states.

Different parameters can be used to define an active state from the structural point of view. The most common is the large-scale displacement (7 Å) of the cytoplasmic side of TM6, observed first by electron paramagnetic resonance [64] and later confirmed in the active structures of rhodopsin [52,53,60–63] and the  $\beta_2$  adrenergic receptor

[33,65]. In the latter, this movement is larger (11–14 Å), possibly due to the binding of intracellular partners (nanobody or G protein).

A second criterion to define an active state is the rearrangement of a “transmission switch” in the TM3–TM5–TM6 interface near the binding site. The influence of Leu125(3.40) on the structure of the proline-induced distortion of TM5 was first proposed for rhodopsin [47], and its functional relevance in other GPCRs was confirmed in the histamine H1 receptor [66]. The concerted action of this residue with Phe261(6.44) during activation was first proposed for the  $\beta_2$  adrenergic receptor [65], and a comparative analysis of active structures lead us to suggest that this transmission switch is a key element of activation and constitutes a common theme of GPCR activation [48]. In summary, rearrangement of the packing between Ile125(3.40), Pro215(5.50), Leu216(5.51) and Phe261(6.44) leads to a weakening of the TM5–TM6 interface and local conformational

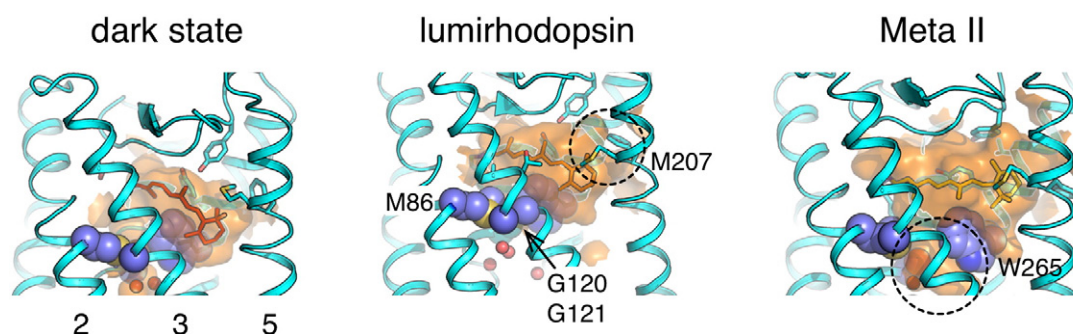


**Fig. 3.** Transition from the inactive dark state to lumirhodopsin results in an increase in the volume of the binding pocket (orange surface), mainly due to the change in the side chain conformation of Met207(5.42) (circle in the center panel). At this stage there is also a small relocation of Met86(2.53). In the transition to Meta II, a larger rearrangement in TM6 results in the opening of a passage towards the cytoplasmic side (circle in the right panel) that allows the relocation of water molecules.

changes at Pro211(5.50), which can be transmitted through TM5 [51]. This transmission switch is not activated in lumirhodopsin, so it must be triggered in later stages of the activation pathway, possibly in Meta I. The residues in the transmission switch are highly conserved in rhodopsin-like GPCRs (Table 2). This suggests that the conformational changes in the TM3–TM5–TM6 interface constitute a conserved activation route in rhodopsin-like GPCRs.

The analysis of these two indicators of the active state (TM6 movement and activation of the transmission switch in TM3–TM5–TM6) in the recent structures of non-rhodopsin GPCRs bound to agonists [33,65,67–73] allows us to hypothesize that some of these structures correspond to intermediates along the activation pathway. Within the framework of rhodopsin activation, a “true” active state (i.e. Meta II) would have to meet the two criteria, while intermediate states, such as Meta I, would only feature an activated transmission switch, without the relocation of TM6.

The structures of  $\beta_1$  adrenergic receptor thermostabilized by mutagenesis and bound to full and partial agonists [73] show small local structural changes in the binding pocket, but they lack both the rearrangement of the transmission switch (Table 2) and the larger relocation of TM6. These structures correspond to the low-affinity non-signaling binding states, formed on initial agonist binding. In this case, the mutations that increase the thermal stability of the protein construct and allowed crystallization, have likely locked the receptor in a conformational state that cannot easily proceed through activation. Thus, in the framework of rhodopsin activation, they most closely resemble a lumirhodopsin-like state, with the agonists establishing a similar weakening effect on interhelical interactions as the  $\beta$ -ionone movement in lumirhodopsin.

The adenosine  $A_{2A}$  receptor has been crystallized in complex with agonists as a fusion protein with T4 lysozyme [72] and thermostabilized by mutagenesis [71]. Both structures feature an activated transmission switch (Table 2), similarly to the active structures of rhodopsin and  $\beta_2$  adrenergic receptor [48], but the movement of the cytoplasmic side of TM6 is significantly smaller (Fig. 4). Thus, the ligand-binding site and the immediate vicinity correspond to an active state, but lysozyme fusion and mutagenesis seem to have decoupled the agonist-induced activation of the transmission switch from the full relocation of TM6 and opening of the G protein-binding site. We have hypothesized that

the agonist-bound  $A_{2A}$  receptor structures resemble a Meta I-like intermediate state that expresses some, but not all, of the conformational changes associated to activation [48]. These structures are “further down” in the activation pathway than in the case of  $\beta_1$  adrenergic receptor, but do not seem to correspond to fully active states.

The neurotensin NTS1 receptor has been crystallized in complex with the C-terminal portion of the cognate agonist neurotensin [69]. In this case, the protein was simultaneously thermostabilized by mutagenesis and fused with T4 lysozyme. Despite being heavily engineered, this structure presents many features of an active state. While there are differences in the composition of the transmission switch (see Table 2), the conformations of M250(5.51) and F317(6.44) correspond to an active state. Also, TM6 is displaced to a similar degree than rhodopsin, opening a cavity for G protein binding (Fig. 4). However, this cavity is occluded by part of TM7. While this may be an artifact of the protein construct, it leads the authors to conclude that this structure does not represent the structure of a fully active receptor.

Finally, the serotonin 5HT<sub>1B</sub> and 5HT<sub>2B</sub> receptors have been crystallized in complex with the agonists ergotamine (5HT<sub>2B</sub>) and dihydroergotamine (5HT<sub>1B</sub> and 5HT<sub>2B</sub>), as fusion proteins with the apocytochrome b(562)RIL [67,68]. In this case, the transmission switch (referred to as the P–I–F motif by the authors) is only fully activated in 5HT<sub>1B</sub>, while 5HT<sub>2B</sub> presents an intermediate state (see Table 2). In both cases, the cytoplasmic side of TM6 is only slightly rearranged, similarly to the adenosine  $A_{2A}$  receptor (Fig. 4). This may be due to the design of the fusion protein, as BRIL forms continuous helical stretches with TM5 and TM6, presumably hampering their rearrangement upon activation. In addition, in one of the 5HT<sub>1B</sub> structures, a loop of b(562)RIL directly contacts the cytoplasmic surface of the receptor. It is thus very likely that these constructs cannot be properly activated by agonists, and are trapped in an intermediate active state, resembling Meta I.

In summary, several of the currently available agonist-bound GPCR crystal structures do not feature all the structural features of an active state (e.g. Meta II [52,61] or  $\beta_2$  adrenergic receptor in complex with a nanobody [65] or a G protein [33]). The  $\beta_1$  adrenergic receptor seems to be trapped in a very early intermediate, possibly resembling lumirhodopsin. The  $A_{2A}$  and serotonin receptors may resemble later intermediates, where some structural changes in the cytoplasmic side have taken place, as in Meta I. The neurotensin NTS1 receptor features a remarkably active-like conformation, but important distortions in TM7 lead us to suggest that this receptor does not represent a fully-active state.

## 5. Conclusions

The constant trickle of non-rhodopsin GPCR structures from 2007 (which seems it can become an avalanche soon) may have led some GPCR researchers to think that we should fully embrace this new and exciting structural information and leave rhodopsin behind. Good old rhodopsin was crucial up to then, as it was the only GPCR for which we had high resolution structural information, but now it seems many have waved it goodbye or simply forgotten it. This may be partially due to the fact that there has always been an invisible divide between “rhodopsin people” and “non-rhodopsin people” in the GPCR field. As a scientist who has learned to have one foot in each side, I can say that rhodopsin still has a lot to teach us about how GPCRs work.

In the Introduction I mentioned the “historic” reasons why rhodopsin has been a key player in this field, and in this paper I described a few examples on how useful information can be extracted from its structures. But rhodopsin is still at the forefront of some aspects in GPCR research, for example in the study of the molecular basis of disease-inducing mutations or of cellular signaling networks at a systems level.

Due to the key role of GPCRs in cellular physiology, mutations that result in defective signaling are linked to more than 30 different human diseases, such as diabetes insipidus, fertility disorders, hypothyroidism, and carcinomas, and more than 700 of such

**Table 2**

Composition of the transmission switch in TM3–TM5–TM6 in GPCRs for which agonist-bound structures have been solved. Green and red denote, respectively, active and inactive conformations of the residues in the switch. The lower section shows the amino acid conservation in this position for Class A (rhodopsin-like) GPCRs. It is worth to note that in the neurotensin NTS1 receptor positions 5.51 and, particularly, 3.40, there is a remarkably different composition (in italics). Position 5.51 in 5HT<sub>1B</sub> also differs from the general trend.

	3.40	5.50	5.51	6.44
Rho	L125	P215	L216	F261
$\beta_1$ AR	I129	P219	L220	F299
$\beta_2$ AR	I121	P211	L212	F282
$A_{2A}$ R	I92	P189	L190	F242
5HT <sub>1B</sub>	I137	P220	T221	F323
5HT <sub>2B</sub>	I143	P229	L230	F333
NTS1R	A157	P249	M250	F317
Class A	I: 41%	P: 77%	L: 45%	F: 80%
	V: 21%		F: 14%	Y: 9%
	L: 19%		V: 13%	
			M: 12%	

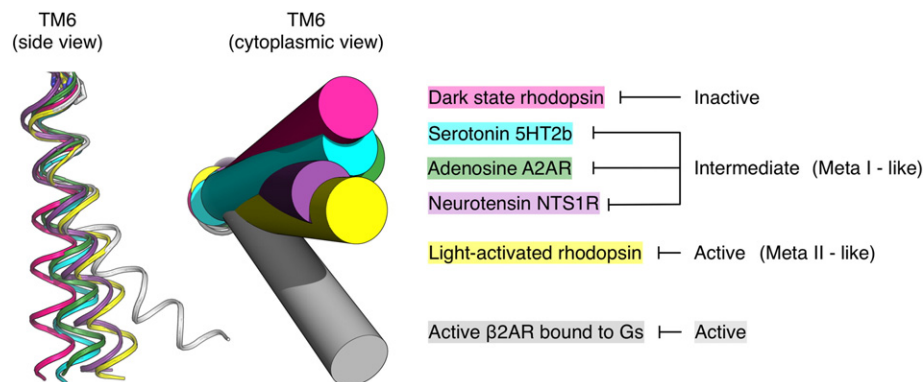


**Fig. 4.** Relative orientation of TM6 in the crystal structures of dark state inactive rhodopsin and agonist-bound GPCRs. In the adenosine A<sub>2A</sub> and serotonin 5HT<sub>2B</sub> receptors, the rearrangement of the cytoplasmic side of TM6 compared to inactive rhodopsin is relatively modest (also in the serotonin 5HT<sub>1B</sub> receptor, not shown for clarity). Thus, this region may resemble a Meta I-like state. While in the neurotensin NTS1 receptor TM6 resembles that of active rhodopsin, other structural features suggest that this structure also represent an intermediate active state (see text).

mutations have been identified [74]. Some of these mutations are located in the transmembrane bundle, and most likely disrupt the structure or the dynamic properties of the receptor, which translates into malfunction and ultimately into disease. In these cases, the structural analysis of these mutants can lead to a better understanding of the molecular basis of the disease, and to the development of new therapeutic strategies. Rhodopsin has been the first (and so far only) GPCR for which the structure of a disease-related mutant (Gly90(2.57)-Asp) has been solved [60]. This structure suggests the molecular mechanisms by which this mutation destabilizes the inactive conformation while selectively favoring a short-lived preactivated conformation, resulting in retinitis pigmentosa or congenital night blindness. Interestingly, this mutation is located at the strong distortion in TM2 (Fig. 2) and creates an unnatural salt bridge between TM2 and TM7. The mutant has a reduced arrestin binding [60], further suggesting the involvement of the TM2/TM7 activation pathway in activation and, possibly, in biased signaling [23].

At a completely different scale, it is increasingly clear that to fully understand GPCR function at the cellular level, we need to unravel the details of the signaling pathways to obtain a comprehensive view of signal transduction. While this is an area of intense research [75], our current understanding of GPCR signaling at a systems level is still relatively limited [76–79]. To date, the most detailed and exhaustive multiscale signal transduction network of a GPCR has been developed for rhodopsin, offering a comprehensive view of signal transduction and suggesting novel signaling routes to vesicular trafficking and cytoskeleton dynamics [80].

Of course, there are still open questions in the field of rhodopsin structural biology that are relevant to GPCR research. For instance, obtaining a high-resolution structure of the Meta I intermediate would complete the structural picture of the rhodopsin activation cycle, which would shed light into the sequence of conformational changes that lead to the stabilization of the active state in rhodopsin-like GPCRs. Also, it is presently unknown if the dissimilarity in the rearrangement of TM6 between the structures of Meta II bound to the GαCT peptide and the β<sub>2</sub> adrenergic receptor bound to Gs (Fig. 4) is due to a fundamental difference in the active conformation of these two receptors, or they simply reflect the effects of the different binding partners present in the crystal structures. While the rhodopsin–GαCT peptide complexes feature all the properties of Meta II, they display a narrower cytoplasmic opening than the active β<sub>2</sub> adrenergic receptor. Obtaining the structure of the complex between rhodopsin and transducin, and comparison with the rhodopsin–GαCT peptide complexes, would allow us to have a better understanding of the role of ligand-induced conformational rearrangement of TM6 on the stabilization of the complex with the G protein. Finally, retinal proteins are likely to play an important role in the development of X-ray free electron laser

(XFEL) crystallography. The fast development of XFEL imaging techniques have allowed the recent structural determination of a membrane protein complex, photosystem I, by merging data from thousands of diffraction images from nanocrystals [81]. As obtaining large and well-diffracting crystals of membrane proteins is particularly challenging, XFEL crystallography represents a very exciting new approach with the potential to revolutionize the field of membrane protein structural biology [82]. But, importantly, the use of an XFEL synchronized with an optical pump laser can be used to obtain diffraction snapshots from photoactivatable membrane proteins [83]. This technique opens the door to time-resolved structural studies of retinal proteins, which would allow us to obtain information of GPCR activation at very high temporal and spatial resolutions.

In summary, rhodopsin remains a relevant player in the field of GPCR research, and it will likely remain so in the future. Definitely, you can teach an old dog new tricks.

## Acknowledgements

I am grateful for the financial support from the Swiss National Science Foundation grants 31003A\_132815 and 31003A\_146520.

## References

- [1] C.G. Tate, G.F.X. Schertler, Engineering G protein-coupled receptors to facilitate their structure determination, *Curr. Opin. Struct. Biol.* 19 (2009) 386–395.
- [2] S. Granier, B.K. Kobilka, A new era of GPCR structural and chemical biology, *Nat. Chem. Biol.* 8 (2012) 670–673.
- [3] A.J. Venkatakrisnan, X. Deupi, G. Lebon, C.G. Tate, G.F. Schertler, M.M. Babu, Molecular signatures of G-protein-coupled receptors, *Nature* 494 (2013) 185–194.
- [4] K. Palczewski, Crystal structure of rhodopsin: a G protein-coupled receptor, *Science* 289 (2000) 739–745.
- [5] J.J. Ruprecht, T. Mielke, R. Vogel, C. Villa, G.F.X. Schertler, Electron crystallography reveals the structure of metarhodopsin I, *EMBO J.* 23 (2004) 3609–3620.
- [6] K.P. Hofmann, P. Scheerer, P.W. Hildebrand, H.-W. Choe, J.H. Park, M. Heck, O.P. Ernst, A G protein-coupled receptor at work: the rhodopsin model, *Trends Biochem. Sci.* 34 (2009) 540–552.
- [7] B. Knierim, K.P. Hofmann, O.P. Ernst, W.L. Hubbell, Sequence of late molecular events in the activation of rhodopsin, *Proc. Natl. Acad. Sci. U. S. A.* 104 (2007) 20290–20295.
- [8] C. Altenbach, A.K. Kusnetzow, O.P. Ernst, K.P. Hofmann, W.L. Hubbell, High-resolution distance mapping in rhodopsin reveals the pattern of helix movement due to activation, *Proc. Natl. Acad. Sci. U. S. A.* 105 (2008) 7439–7444.
- [9] D.L. Farrens, What site-directed labeling studies tell us about the mechanism of rhodopsin activation and G-protein binding, *Photochem. Photobiol. Sci.* 9 (2010) 1466–1474.
- [10] M. Murakami, T. Kouyama, Crystallographic analysis of the primary photochemical reaction of squid rhodopsin, *J. Mol. Biol.* 413 (2011) 615–627.
- [11] H. Nakamichi, T. Okada, Local peptide movement in the photoreaction intermediate of rhodopsin, *Proc. Natl. Acad. Sci. U. S. A.* 103 (2006) 12729–12734.
- [12] H. Nakamichi, T. Okada, Crystallographic analysis of primary visual photochemistry, *Angew. Chem. Int. Ed.* 45 (2006) 4270–4273.



- [13] S. Ahuja, E. Crocker, M. Eilers, V. Hornak, A. Hirshfeld, M. Ziliox, N. Syrett, P.J. Reeves, H.G. Khorana, M. Sheves, S.O. Smith, Location of the retinal chromophore in the activated state of rhodopsin\*, *J. Biol. Chem.* 284 (2009) 10190–10201.
- [14] J.A. Gonçalves, K. South, S. Ahuja, E. Zaitseva, C.A. Opefi, M. Eilers, R. Vogel, P.J. Reeves, S.O. Smith, Highly conserved tyrosine stabilizes the active state of rhodopsin, *Proc. Natl. Acad. Sci. U. S. A.* 107 (2010) 19861–19866.
- [15] A.V. Struts, G.F.J. Salgado, M.F. Brown, Solid-state  $^2\text{H}$  NMR relaxation illuminates functional dynamics of retinal cofactor in membrane activation of rhodopsin, *Proc. Natl. Acad. Sci. U. S. A.* 108 (2011) 8263–8268.
- [16] X. Ding, X. Zhao, A. Watts, G-protein-coupled receptor structure, ligand binding and activation as studied by solid-state NMR spectroscopy, *Biochem. J.* 450 (2013) 443–457.
- [17] S. Muralidharan, G.M. Maher, W.A. Boyle, J.M. Nerbonne, “Caged” phenylephrine: development and application to probe the mechanism of  $\alpha$ -receptor-mediated vasoconstriction, *Proc. Natl. Acad. Sci. U. S. A.* 90 (1993) 5199–5203.
- [18] W.A. Boyle, S. Muralidharan, G.M. Maher, J.M. Nerbonne, Vascular actions of “caged” phenylephrine analogs depend on the structure and site of attachment of the 2-nitrobenzyl group, *J. Photochem. Photobiol. B Biol.* 41 (1997) 233–244.
- [19] D.R. Madden, S. Thiran, H. Zimmermann, J. Romm, V. Jayaraman, Stereochemistry of quinoxaline antagonist binding to a glutamate receptor investigated by Fourier transform infrared spectroscopy, *J. Biol. Chem.* 276 (2001) 37821–37826.
- [20] A. Barth, Phosphoenzyme conversion of the sarcoplasmic reticulum  $\text{Ca}^{2+}$ -ATPase molecular interpretation of infrared difference spectra, *J. Biol. Chem.* 274 (1999) 22170–22175.
- [21] C. Kötting, A. Kallenbach, Y. Suveyzdis, C. Eichholz, K. Gerwert, Surface change of Ras enabling effector binding monitored in real time at atomic resolution, *ChemBioChem* 8 (2007) 781–787.
- [22] M.P. Bokoch, Y. Zou, S.G.F. Rasmussen, C.W. Liu, R. Nygaard, D.M. Rosenbaum, J.J. Fung, H.-J. Choi, F.S. Thian, T.S. Kobilka, J.D. Puglisi, W.I. Weis, L. Pardo, R.S. Prosser, L. Mueller, B.K. Kobilka, Ligand-specific regulation of the extracellular surface of a G-protein-coupled receptor, *Nature* 463 (2010) 108–112.
- [23] J.J. Liu, R. Horst, V. Katritch, R.C. Stevens, K. Wüthrich, Biased signaling pathways in  $\beta_2$ -adrenergic receptor characterized by  $^{19}\text{F}$ -NMR, *Science* 335 (2012) 1106–1110.
- [24] R. Nygaard, Y. Zou, R.O. Dror, T.J. Mildorf, D.H. Arlow, A. Manglik, A.C. Pan, C.W. Liu, J.J. Fung, M.P. Bokoch, F.S. Thian, T.S. Kobilka, D.E. Shaw, L. Mueller, R.S. Prosser, B.K. Kobilka, The dynamic process of  $\beta_2$ -adrenergic receptor activation, *Cell* 152 (2013) 532–542.
- [25] Y. Kokufu, T. Ueda, J. Okude, Y. Shiraishi, K. Kondo, M. Maeda, H. Tsujishita, I. Shimada, Efficacy of the  $\beta_2$ -adrenergic receptor is determined by conformational equilibrium in the transmembrane region, *Nat. Commun.* 3 (2012) 1045.
- [26] H. Unal, S.S. Karnik, Domain Coupling in GPCRs: The Engine for Induced Conformational Changes, *Trends Pharmacol. Sci.* 33 (2012) 79–88, <http://dx.doi.org/10.1016/j.tips.2011.09.007>.
- [27] V.-P.P. Jaakola, J. Prilusky, J.L. Sussman, A. Goldman, G protein-coupled receptors show unusual patterns of intrinsic unfolding, *Protein Eng. Des. Sel.* 18 (2005) 103–110.
- [28] M.M. Babu, R.W. Kriwacki, R.V. Pappu, Structural biology. Versatility from protein disorder, *Science* 337 (2012) 1460–1461.
- [29] S.G.F. Rasmussen, H.-J. Choi, D.M. Rosenbaum, T.S. Kobilka, F.S. Thian, P.C. Edwards, M. Burghammer, V.R.P. Ratnala, R. Sanishvili, R.F. Fischetti, G.F.X. Schertler, W.I. Weis, B.K. Kobilka, Crystal structure of the human  $\beta_2$  adrenergic G-protein-coupled receptor, *Nature* 450 (2007) 383–387.
- [30] W. Liu, E. Chun, A.A. Thompson, P. Chubukov, F. Xu, V. Katritch, G.W. Han, C.B. Roth, L.H. Heitman, A.P. Iljerman, V. Cherezov, R.C. Stevens, Structural basis for allosteric regulation of GPCRs by sodium ions, *Science* 337 (2012) 232–235.
- [31] R. Moukhametzanov, T. Warne, P.C. Edwards, M.J. Serrano-Vega, A.G.W. Leslie, C.G. Tate, G.F.X. Schertler, Two distinct conformations of helix 6 observed in antagonist-bound structures of a  $\beta_1$ -adrenergic receptor, *Proc. Natl. Acad. Sci. U. S. A.* 108 (2011) 8228–8232.
- [32] Y. Zou, W.I. Weis, B.K. Kobilka, N-Terminal T4 lysozyme fusion facilitates crystallization of a G protein coupled receptor, *PLoS One* 7 (2012) e46039.
- [33] S.G.F. Rasmussen, B.T. Devree, Y. Zou, A.C. Kruse, K.Y. Chung, T.S. Kobilka, F.S. Thian, P.S. Chae, E. Pardon, D. Calinski, J.M. Mathiesen, S.T.A. Shah, J.A. Lyons, M. Caffrey, S.H. Gellman, J. Steyaert, G. Skiniotis, W.I. Weis, R.K. Sunahara, B.K. Kobilka, Crystal structure of the  $\beta_2$  adrenergic receptor-Gs protein complex, *Nature* 477 (2011) 549–555.
- [34] A.L. Lomize, I.D. Pogozheva, M.A. Lomize, H.I. Mosberg, Positioning of proteins in membranes: a computational approach, *Protein Sci.* 15 (2006) 1318–1333.
- [35] A.S. Doré, N. Robertson, J.C. Errey, I. Ng, K. Hollenstein, B. Tehan, E. Hurrell, K. Bennett, M. Congreve, F. Magnani, C.G. Tate, M. Weir, F.H. Marshall, Structure of the adenosine A(2A) receptor in complex with ZM241385 and the xanthines XAC and caffeine, *Structure* 19 (2011) 1283–1293.
- [36] T. Hino, T. Arakawa, H. Iwanari, T. Yurugi-Kobayashi, C. Ikeda-Suno, Y. Nakada-Nakura, O. Kusano-Arai, S. Weyand, T. Shimamura, N. Nomura, A.D. Cameron, T. Kobayashi, T. Hamakubo, S. Iwata, T. Murata, G-protein-coupled receptor inactivation by an allosteric inverse-agonist antibody, *Nature* 482 (2012) 237–240, <http://dx.doi.org/10.1038/nature10750>.
- [37] J. Li, P.C. Edwards, M. Burghammer, C. Villa, G.F.X. Schertler, Structure of bovine rhodopsin in a trigonal crystal form, *J. Mol. Biol.* 343 (2004) 1409–1438.
- [38] M. Murakami, T. Kouyama, Crystal structure of squid rhodopsin, *Nature* 453 (2008) 363–367.
- [39] G. Bellot, S. Granier, W. Bourguet, R. Seyer, R. Rahmeh, B. Mouillac, R. Pascal, C. Mendre, H. Déné, Structure of the third intracellular loop of the vasopressin V2 receptor and conformational changes upon binding to gC1qR, *J. Mol. Biol.* 388 (2009) 491–507.
- [40] K. Haga, A.C. Kruse, H. Asada, T. Yurugi-Kobayashi, M. Shiroishi, C. Zhang, W.I. Weis, T. Okada, B.K. Kobilka, T. Haga, T. Kobayashi, Structure of the human M2 muscarinic acetylcholine receptor bound to an antagonist, *Nature* 482 (2012) 547–551.
- [41] A.C. Kruse, J. Hu, A.C. Pan, D.H. Arlow, D.M. Rosenbaum, E. Rosemond, H.F. Green, T. Liu, P.S. Chae, R.O. Dror, D.E. Shaw, W.I. Weis, J. Wess, B.K. Kobilka, Structure and dynamics of the M3 muscarinic acetylcholine receptor, *Nature* 482 (2012) 552–556.
- [42] S. Ichijima, Y. Oka, K. Haga, S. Kojima, Y. Tateishi, M. Shirakawa, T. Haga, The structure of the third intracellular loop of the muscarinic acetylcholine receptor M2 subtype, *FEBS Lett.* 580 (2006) 23–26.
- [43] R. Rahmeh, M. Damian, M. Cottet, H. Orcel, C. Mendre, T. Durroux, K.S. Sharma, G. Durand, B. Pucci, E. Trinquet, J.M. Zwier, X. Deupi, P. Bron, J.-L. Baneres, B. Mouillac, S. Granier, Structural insights into biased G protein-coupled receptor signaling revealed by fluorescence spectroscopy, *Proc. Natl. Acad. Sci. U. S. A.* 109 (2012) 6733–6738.
- [44] X. Deupi, Quantification of structural distortions in the transmembrane helices of GPCRs, *Methods Mol. Biol.* 914 (2012) 219–235.
- [45] M. Bansal, S. Kumar, R. Velavan, HELANAL: a program to characterize helix geometry in proteins, *J. Biomol. Struct. Dyn.* 17 (2000) 811–819.
- [46] J.A. Ballesteros, H. Weinstein, Integrated methods for the construction of three-dimensional models and computational probing of structure-function relations in G protein-coupled receptors, *Methods Neurosci.* (1995) 366–428.
- [47] X. Deupi, N. Dölkner, M.L. López-Rodríguez, M. Campillo, J.A. Ballesteros, L. Pardo, Structural models of class A G protein-coupled receptors as a tool for drug design: insights on transmembrane bundle plasticity, *Curr. Top. Med. Chem.* 7 (2007) 991–998.
- [48] X. Deupi, J. Standfuss, Structural insights into agonist-induced activation of G-protein-coupled receptors, *Curr. Opin. Struct. Biol.* 21 (2011) 541–551.
- [49] S. Madabushi, A.K. Gross, A. Philippi, E.C. Meng, T.G. Wensel, O. Lichtarge, Evolutionary trace of G protein-coupled receptors reveals clusters of residues that determine global and class-specific functions, *J. Biol. Chem.* 279 (2004) 8126–8132.
- [50] G.J. Rodriguez, R. Yao, O. Lichtarge, T.G. Wensel, Evolution-guided discovery and recoding of allosteric pathway specificity determinants in psychoactive bioamine receptors, *Proc. Natl. Acad. Sci. U. S. A.* 107 (2010) 7787–7792.
- [51] X. Deupi, J. Standfuss, G.F.X. Schertler, Conserved activation pathways in G-protein-coupled receptors, *Biochem. Soc. Trans.* 40 (2012) 383–388.
- [52] X. Deupi, P.C. Edwards, A. Singhal, B. Nickle, D.D. Oprian, G.F.X. Schertler, J. Standfuss, Stabilized G protein binding site in the structure of constitutively active metarhodopsin-II, *Proc. Natl. Acad. Sci. U. S. A.* 109 (2012) 119–124.
- [53] J. Standfuss, P.C. Edwards, A. D'Antona, M. Fransen, G. Xie, D.D. Oprian, G.F.X. Schertler, The structural basis of agonist-induced activation in constitutively active rhodopsin, *Nature* 471 (2011) 656–660.
- [54] M.M. Rosenkilde, T. Benned-Jensen, T.M. Frimurer, T.W. Schwartz, The minor binding pocket: a major player in 7TM receptor activation, *Trends Pharmacol. Sci.* 31 (2010) 567–574.
- [55] B.K. Kobilka, The structural basis of G-protein-coupled receptor signaling (Nobel lecture), *Angew. Chem. Int. Ed.* 52 (2013) 6380–6388.
- [56] S. Bockenhauer, A. Fürstner, X.J. Yao, B.K. Kobilka, W.E. Moerner, Conformational dynamics of single G protein-coupled receptors in solution, *J. Phys. Chem. B* 115 (2011) 13328–13338.
- [57] X. Deupi, B.K. Kobilka, Energy landscapes as a tool to integrate GPCR structure, dynamics, and function, *Physiology (Bethesda)* 25 (2010) 293–303.
- [58] M. Ambrosio, A. Zürn, M.J. Lohse, Sensing G protein-coupled receptor activation, *Neuropharmacology* 60 (2011) 45–51.
- [59] S. Ye, E. Zaitseva, G. Caltabiano, G.F.X. Schertler, T.P. Sakmar, X. Deupi, R. Vogel, Tracking G-protein-coupled receptor activation using genetically encoded infrared probes, *Nature* 464 (2010) 1386–1389.
- [60] A. Singhal, M.K. Ostermaier, S.A. Vishnivetskiy, V. Panneels, K.T. Homan, J.J.G. Tesmer, D. Veprintsev, X. Deupi, V.V. Gurevich, G.F.X. Schertler, J. Standfuss, Insights into congenital stationary night blindness based on the structure of G90D rhodopsin, *EMBO Rep.* 14 (2013) 520–526.
- [61] H.-W. Choe, Y.J. Kim, J.H. Park, T. Morizumi, E.F. Pai, N. Krauß, K.P. Hofmann, P. Scheerer, O.P. Ernst, Crystal structure of metarhodopsin II, *Nature* 471 (2011) 651–655.
- [62] P. Scheerer, J.H. Park, P.W. Hildebrand, Y.J. Kim, N. Krauß, H.-W. Choe, K.P. Hofmann, O.P. Ernst, Crystal structure of opsin in its G-protein-interacting conformation, *Nature* 455 (2008) 497–502.
- [63] J.H. Park, P. Scheerer, K.P. Hofmann, H.-W. Choe, O.P. Ernst, Crystal structure of the ligand-free G-protein-coupled receptor opsin, *Nature* 454 (2008) 183–187.
- [64] D.L. Farrens, C. Altenbach, K. Yang, W.L. Hubbell, H.G. Khorana, Requirement of rigid-body motion of transmembrane helices for light activation of rhodopsin, *Science* 274 (1996) 768–770.
- [65] S.G.F. Rasmussen, H.-J. Choi, J.J. Fung, E. Pardon, P. Casarosa, P.S. Chae, B.T. Devree, D.M. Rosenbaum, F.S. Thian, T.S. Kobilka, A. Schnapp, I. Konetzki, R.K. Sunahara, S.H. Gellman, A. Pautsch, J. Steyaert, W.I. Weis, B.K. Kobilka, Structure of a nanobody-stabilized active state of the  $\beta_2$  adrenoceptor, *Nature* 469 (2010) 175–180.
- [66] K. Sansuk, X. Deupi, I.R. Torrecillas, A. Jongejan, S. Nijmeijer, R.A. Bakker, L. Pardo, R. Leurs, A structural insight into the reorientation of transmembrane domains 3 and 5 during family A G protein-coupled receptor activation, *Mol. Pharmacol.* 79 (2011) 262–269.
- [67] C. Wang, Y. Jiang, J. Ma, H. Wu, D. Wacker, V. Katritch, G.W. Han, W. Liu, X.-P. Huang, E. Vardy, J.D. McCorvy, X. Gao, X.E. Zhou, K. Melcher, C. Zhang, F. Bai, H. Yang, L. Yang, H. Jiang, B.L. Roth, et al., Structural basis for molecular recognition at serotonin receptors, *Science* 340 (2013) 610–614.



- [68] D. Wacker, C. Wang, V. Katritch, G.W. Han, X.-P. Huang, E. Vardy, J.D. McCorvy, Y. Jiang, M. Chu, F.Y. Siu, W. Liu, H.E. Xu, V. Cherezov, B.L. Roth, R.C. Stevens, Structural features for functional selectivity at serotonin receptors, *Science* 340 (2013) 615–619.
- [69] J.F. White, N. Noinaj, Y. Shibata, J. Love, B. Kloss, F. Xu, J. Gvozdenovic-Jeremic, P. Shah, J. Shiloach, C.G. Tate, R. Grisshammer, Structure of the agonist-bound neurotensin receptor, *Nature* 490 (2012) 508–513.
- [70] T. Warne, P.C. Edwards, A.G.W. Leslie, C.G. Tate, Crystal structures of a stabilized  $\beta(1)$ -adrenoceptor bound to the biased agonists bucindolol and carvedilol, *Structure* 20 (2012) 841–849.
- [71] G. Lebon, T. Warne, P.C. Edwards, K. Bennett, C.J. Langmead, A.G.W. Leslie, C.G. Tate, Agonist-bound adenosine A2A receptor structures reveal common features of GPCR activation, *Nature* 474 (2011) 521–525.
- [72] F. Xu, H. Wu, V. Katritch, G.W. Han, K.A. Jacobson, Z.-G. Gao, V. Cherezov, R.C. Stevens, Structure of an agonist-bound human A2A adenosine receptor, *Science* 332 (2011) 322–327.
- [73] T. Warne, R. Moukhametziev, J.G. Baker, R. Nehmé, P.C. Edwards, A.G.W. Leslie, G.F.X. Schertler, C.G. Tate, The structural basis for agonist and partial agonist action on a  $\beta(1)$ -adrenergic receptor, *Nature* 469 (2010) 241–244.
- [74] T. Schöneberg, A. Schulz, H. Biebertmann, T. Hermsdorf, H. Römpler, K. Sangkuhl, Mutant G-protein-coupled receptors as a cause of human diseases, *Pharmacol. Ther.* 104 (2004) 173–206.
- [75] A.C. Magalhaes, H. Dunn, S.S.G. Ferguson, Regulation of GPCR activity, trafficking and localization by GPCR-interacting proteins, *Br. J. Pharmacol.* 165 (2012) 1717–1736.
- [76] K. Xiao, J.-P. Sun, J. Kim, S. Rajagopal, B. Zhai, J. Villén, W. Haas, J.J. Kovacs, A.K. Shukla, M.R. Hara, M. Hernandez, A. Lachmann, S. Zhao, Y. Lin, Y. Cheng, K. Mizuno, A. Ma'ayan, S.P. Gygi, R.J. Lefkowitz, Global phosphorylation analysis of beta-arrestin-mediated signaling downstream of a seven transmembrane receptor (7TMR), *Proc. Natl. Acad. Sci. U. S. A.* 107 (2010) 15299–15304.
- [77] G.L. Christensen, C.D. Kelstrup, C. Lyngsø, U. Sarwar, R. Bøgebo, S.P. Sheikh, S. Gammeltoft, J.V. Olsen, J.L. Hansen, Quantitative phosphoproteomics dissection of seven-transmembrane receptor signaling using full and biased agonists, *Mol. Cell Proteomics* 9 (2010) 1540–1553.
- [78] D. Heitzler, G. Durand, N. Gallay, A. Rizk, S. Ahn, J. Kim, J.D. Violin, L. Dupuy, C. Gauthier, V. Piketty, P. Crépieux, A. Poupon, F. Clément, F. Fages, R.J. Lefkowitz, E. Reiter, Competing G protein-coupled receptor kinases balance G protein and  $\beta$ -arrestin signaling, *Mol. Syst. Biol.* 8 (2012) 590.
- [79] T. Verano-Braga, V. Schwämmle, M. Sylvester, D.G. Passos-Silva, A.A.B. Peluso, G.M. Etelvino, R.A.S. Santos, P. Roepstorff, Time-resolved quantitative phosphoproteomics: new insights into angiotensin-(1–7) signaling networks in human endothelial cells, *J. Proteome Res.* 11 (2012) 3370–3381, <http://dx.doi.org/10.1021/pr3001755>.
- [80] C. Kiel, A. Vogt, A. Campagna, A. Chatr-aryamontri, M. Swiatek-de Lange, M. Beer, S. Bolz, A.F. Mack, N. Kinkl, G. Cesareni, L. Serrano, M. Ueffing, Structural and functional protein network analyses predict novel signaling functions for rhodopsin, *Mol. Syst. Biol.* 7 (2011).
- [81] H.N. Chapman, P. Fromme, A. Barty, T.A. White, R.A. Kirian, A. Aquila, M.S. Hunter, J. Schulz, D.P. DePonte, U. Weierstall, R.B. Doak, F.R.N.C. Maia, A.V. Martin, I. Schlichting, L. Lomb, N. Coppola, R.L. Shoeman, S.W. Epp, R. Hartmann, D. Rolles, et al., Femtosecond X-ray protein nanocrystallography, *Nature* 470 (2011) 73–77.
- [82] R. Neutze, K. Moffat, Time-resolved structural studies at synchrotrons and X-ray free electron lasers: opportunities and challenges, *Curr. Opin. Struct. Biol.* 22 (2012) 651–659.
- [83] A. Aquila, M.S. Hunter, R.B. Doak, R.A. Kirian, P. Fromme, T.A. White, J. Andreasson, D. Arnlund, S. Bajt, T.R.M. Barends, M. Barthelmess, M.J. Bogan, C. Bostedt, H. Bottin, J.D. Bozek, C. Caleman, N. Coppola, J. Davidsson, D.P. DePonte, V. Elser, et al., Time-resolved protein nanocrystallography using an X-ray free-electron laser, *Opt. Express* 20 (2012) 2706–2716.